Preparation and luminescence properties of Pb²⁺ and Mn²⁺ co-doped Zn₂SiO₄ based on mesoporous silica

LINGYAN DANG[1,*], ZHENFENG NIU[1], JINGRUN GAO[1], XIAOLU QI[1], RUI SHI[1], YAXIN ZHANG[1],
ZHENXING YANG[1,*], QINGSHAN LU[2]
¹College of Sciences, Hebei North University, Zhangjiakou, 075000, China
²School of Physical Science and Technology and Inner Mongolia Key Laboratory of Nanoscience & Nanotechnology, Inner Mongolia University, 010000, China

Pb²⁺ and Mn²⁺ co-doped Zn₂SiO₄ phosphors were prepared by hydrothermal treatment using mesoporous silica as template and silicon source. The reaction temperature is reduced due to the mesoporous structure of mesoporous silica, and the large specific surface area of mesoporous silica is in favor of the uniform doping of ions. The effect of Pb²⁺ on the structure and morphology of Zn₂SiO₄:Mn²⁺ was investigated through various analytical techniques. Excitation and emission spectrum analysis reveals that the increased luminous intensity of Mn²⁺ ions is detected by ion co-doping, which is caused by energy transfer from the Pb²⁺ ion to the Mn²⁺ ion.

1. Introduction

Inorganic phosphors have received a lot of interest due to their high luminescence efficiency, strong chemical and thermal stabilities, and widespread application in the field of light emitting devices. The study of rare-earth or transition metal (TM) ions co-doped host matrix is a potential field for further investigation. The primary lattice luminescence characteristics may be greatly influenced by dopant interaction, which offers an opportunity to develop novel luminescence materials [1]. Recently, Zn₂SiO₄ has aroused researchers' interest as a key matrix material for rare earth and TM ions. Because of high luminescence efficiency and outstanding chemical and thermal stabilities, Zn₂SiO₄ has been widely employed as a host material in the field of phosphors for light emitting devices [2,3]. When Zn₂SiO₄ doped with some specific TM ions such as Mn²⁺, Co²⁺ and so on, green and blue light can be emitted, respectively [4,5]. Among these known inorganic phosphors, manganese-doped zinc silicate (Zn₂SiO₄:Mn²⁺) is a highly efficient green phosphor that is widely used in opto-electronic devices [6-8]. Traditionally, Zn₂SiO₄:Mn²⁺ phosphors are prepared by solid-state reaction method with the calcination temperature above 1300 °C [4,8]. However, this approach encounters the unpredictable distribution of doping ions, high calcination temperatures, prolonged reaction times and the aggregation phosphor particles, which deteriorate the luminescent properties of the phosphors. In addition, other techniques have also been developed, including sol-gel synthesis, which is a solution-based synthesis approach [6], and sol-gel method combined with furnace firing [9]. Nevertheless, because the sol-gel

process's precursor solution reactions are carried out at low reaction temperatures (~75-80 °C), resulting in products with high crystallinity and nanometer-sized particles. In our previous work, Ba²⁺ and Mn²⁺ co-doped Zn₂SiO₄ was obtained by mesoporous template route at a hydrothermal temperature of 250 °C which is lower than the temperature of 360 °C reported by Yoon [10]. This route exhibits a significant advantage of much lower reaction temperature. In this case, the green emission intensity can be effectively tuned with the Ba²⁺ doping concentration [11].

The optical properties of Pb²⁺ have been studied as an activator or in the host matrix. The luminescence properties of the Pb²⁺ ion with 6s² configuration are attributed to the ground state ¹S₀ and two excited states of singlet ¹P₁ and triplet ³P₀,₁,₂ [12-14]. The optical and electronic properties of Pb²⁺ compounds have recently been explored in various applications, such as Pb²⁺-based perovskite [15], white-light emitting material [16], and luminescent sensing [17]. Recently, ZnB₂O₄ doped with Pb²⁺ has been shown to exhibit suppressed concentration quenching phenomenon [14]. Based on this finding, it would be interesting to explore the luminescence properties of Mn²⁺, Pb²⁺ co-doped Zn₂SiO₄ prepared through mesoporous template route with hydrothermal method, which might provide new luminescent materials having potential applications in optical devices.

In this study, Pb²⁺, Mn²⁺ co-doped Zn₂SiO₄ luminescent materials were prepared by hydrothermal method and employing mesoporous silica as a template and silicon source. As far as we know, there has no report on Pb²⁺, Mn²⁺ co-doped Zn₂SiO₄ prepared by the hydrothermal

method. The structural, morphology and optical photoluminescence (PL) of Pb^{2+} and Mn^{2+} co-doped Zn$_2$SiO$_4$ phosphors have been investigated. This approach provides an advantage over alternative strategies in achieving the low temperature preparation and uniform doping of ions.

2. Experimental

2.1. Preparation process

For the preparation of Zn$_{1.94-x}$Pb$_x$Mn$_{0.06}$SiO$_4$ (0.04≤x≤0.10), zinc nitrate hexahydrate, manganese acetate tetrahydrate and lead nitrate with stoichiometric ratio were dissolved in deionized water and stirred at room temperature. Then a certain amount of mesoporous silica was added into the above solution and continually stirred until completely dispersed. After that, 1.33 M of NaOH solution was added and the pH value of the solution was kept at 10. The suspension was further stirred vigorously for about 1 h, transferred to an autoclave and hydrothermally treated at 250 °C for 20 h. Finally, the product was separated from the solution by centrifugation, washed with deionized water to neutral and dried at 60°C to obtain a white powdered sample.

2.2. Analytical characterization

XRD patterns were recorded by using a PANalytical Empyrean X-ray diffractometer with Cu Kα radiation under a θ-2θ scanning mode at 40 kV and 40 mA. The morphology and microstructure were analyzed using a Magellan 400 field emission SEM at 5.00 kV and a JEM-2200 FS field

emission TEM at 200 kV, respectively. PL spectra were recorded on a Hitachi F-7000 spectrophotometer.

3. Results and discussion

3.1. XRD analysis

The XRD patterns of Pb^{2+} and Mn^{2+} co-doped Zn$_2$SiO$_4$ with different Pb^{2+} doping concentrations are displayed in Fig. 1. All the samples show similar diffraction patterns and the peaks can be attributed to the diffractions of the pure willemite Zn$_2$SiO$_4$ [18]. The sharp and intense diffraction peaks indicate that all the samples have high crystallinity. Because of the relatively low doping and the homogeneous mixing of the pre-synthesized solution using mesoporous silica as silicon source, no characteristic peaks of impurity phase have been detected even at a high doping level of x=0.1, suggesting that the Pb^{2+} and Mn^{2+} can be completely dissolved into Zn$_2$SiO$_4$ host lattice by substitution for Zn^{2+} [18]. In our current study, the hydrothermal procedure is facile to obtain pure phases of Zn$_2$SiO$_4$ with high homogeneity and crystallinity. The hydrothermal synthesis temperature is 250 °C, which is lower than that reported value for the hydrothermal synthesis of Mn-doped Zn$_2$SiO$_4$ in rods at 280 °C [19] and considerably greatly lower than the solid-state reaction temperature of 1300 °C [4,8]. This is owing to the porous structure and large specific surface area of mesoporous silica, which leads to a significant increase in reaction active sites and reactant interfaces, facilitating homogenous ion doping.
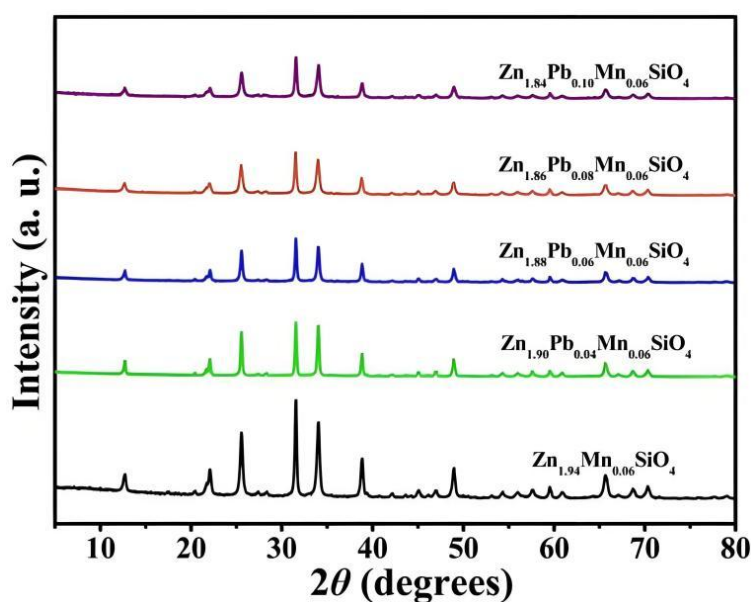
Fig. 1. Wide-angle XRD patterns of Zn$_{1.94-x}$Pb$_x$Mn$_{0.06}$SiO$_4$ with different Pb^{2+} concentrations (colour online)

3.2. Morphology, microstructure and energy spectrum analysis

The size, morphology and microstructure of the samples were investigated using SEM and TEM. Fig. 2a shows the SEM images of $Zn_{1.90}Pb_{0.04}Mn_{0.06}SiO_4$ samples with different resolutions. The samples have nanorod shape and show a smooth surface with a hierarchical structure. This suggests that the sample retains the morphological properties of the mesoporous silica [20]. The samples show an average length up to 600 nm and a mean diameter around 30 nm, showing a length/diameter ratio of approximately 20 (Fig. 2b). The microstructure of the $Zn_{1.90}Pb_{0.04}Mn_{0.06}SiO_4$ was measured by TEM, as shown in Fig. 2c, the images show a bundle-like structure, and side-by-side rods were aligned along the channel direction of the mesoporous silica, which is consistent with the SEM observations. According to energy dispersive spectroscopy (EDS) (Fig. 2d), all content related elements namely Zn, O, Si and dopants Mn, Pb were evidently detected at the chosen positions in SEM images. The existence of the carbon (C) and copper (Cu) peak is due to the supporting carbon film and copper network, respectively. The results demonstrated the doping of Pb^{2+} into the Zn_2SiO_4 lattice to form pure Pb^{2+} and Mn^{2+} co-doped Zn_2SiO_4.
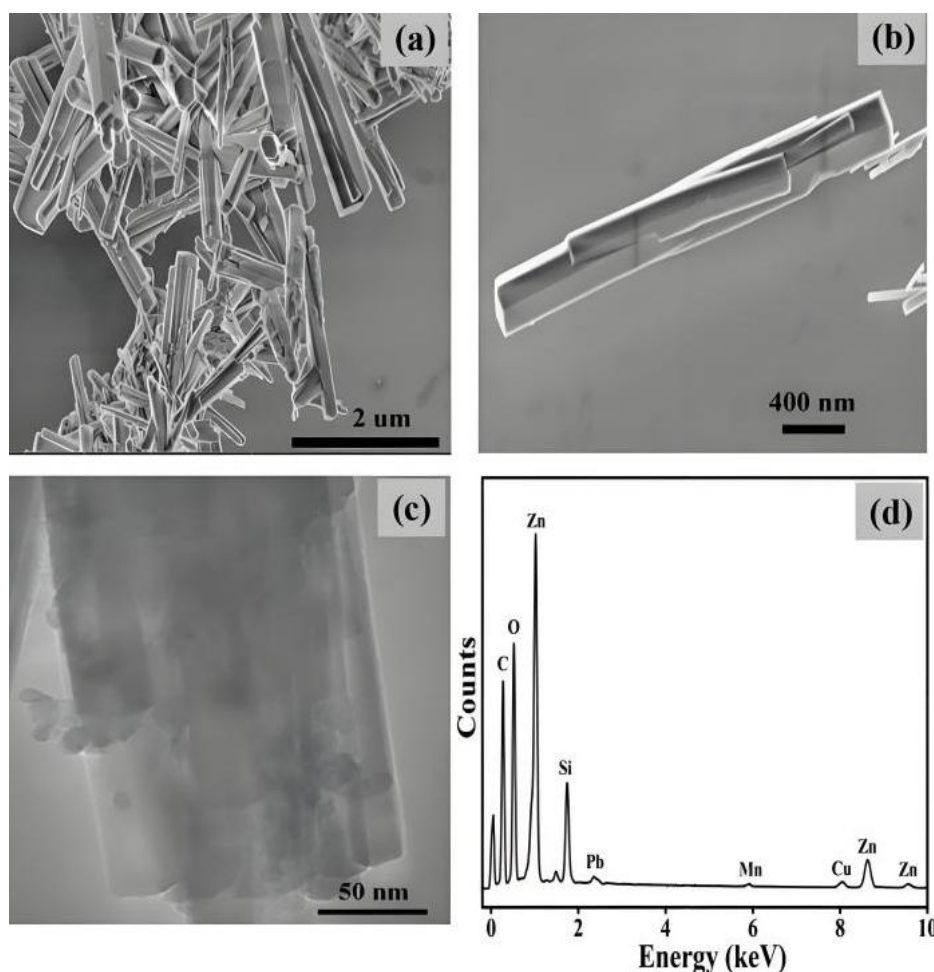
Fig. 2. (a-b) SEM micrographs of $Zn_{1.90}Pb_{0.04}Mn_{0.06}SiO_4$, (c) TEM images of $Zn_{1.90}Pb_{0.04}Mn_{0.06}SiO_4$ and (f) EDS spectra

3.3. Excitation and emission spectroscopy analysis

Fig. 3 shows the excitation spectra of $Zn_{1.94-x}Pb_xMn_{0.06}SiO_4$ with various Pb^{2+} concentrations, which was recorded with an emission wavelength of 520 nm. For the co-doped sample, the excitation peaks show similar characteristics of a broad excitation band at 235 nm with various concentrations of Pb^{2+} ions. By comparing the shapes of the curves in the graphs, it is clearly observed that the excitation spectra of the co-doped sample is almost the same as that of the Mn^{2+} doped sample. However, the luminescence intensities change with increasing the concentration of Pb^{2+} in Zn_2SiO_4. The luminescence intensity of the doped sample with a Pb^{2+} ion doping concentration of 0.04 is the highest in all the doped samples. This may be due to the introduction of the energy levels in the forbidden band, which coincides with the Pb^{2+} doping, causing Mn^{2+} ion dipole e to t_2 jumps [21]. The excitation

spectra of the samples are strongly correlated with their energy band gaps. It also shows that the band gap of Mn^{2+}-doped Zn_2SiO_4 has been significantly altered by Pb^{2+} ions.

As a result, it exhibits very distinct luminescence properties in the presence of the Pb^{2+} ion.
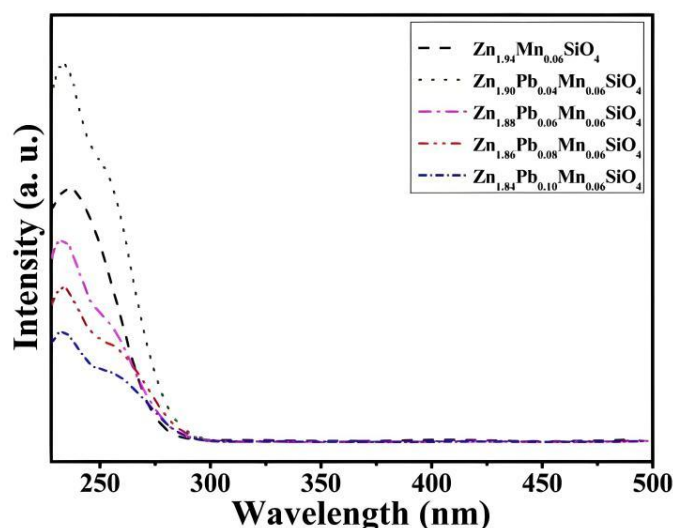
Fig. 3. Excitation spectra of $Zn_{1.94-x}Pb_xMn_{0.06}SiO_4$ with various Pb^{2+} ion concentrations (colour online)

The emission spectra and intensity variation with various doping concentrations is shown in Fig. 4, the excitation wavelength is 235 nm. The brightness of the emission from the phosphor particles is highly dependent on the Pb^{2+} doping concentration. Moreover, the positions of the emission peaks do not change at a fixed excitation wavelength. It can be seen from Fig. 4a, the emission peak of Mn-doped Zn_2SiO_4 phosphors has no change when the Pb^{2+} is co-doped. A single broad emission peak at 520 nm is obtained when excitation wavelength located at 235 nm, which is due to the electronic jump of the manganese ion from $^4T_1(4G)$ to $^6A_1(4G)$ in Zn_2SiO_4. This result is in agreement with previous reported results [22-24]. In Mn^{2+}-doped Zn_2SiO_4, the radius of the Mn^{2+} ion (0.80 Å) and Zn^{2+} (0.74 Å) is very similar and the Mn^{2+} ions take the place of the Zn^{2+} ions and act as the luminescence centers [23]. Meanwhile, the radius of the Pb^{2+} ion is 1.20 Å, which is much larger than the radius of the Zn^{2+} and Mn^{2+} ions, making it is difficult for the Pb^{2+} ion to take the place of the Zn^{2+} ion in the lattice. Thus, most of the Pb^{2+} ions are assumed to be interstitial ions in $Zn_2SiO_4:Mn^{2+}$, Pb^{2+}. The dependence of the emission intensity on the Pb^{2+} doping concentration is shown in Fig. 4b.
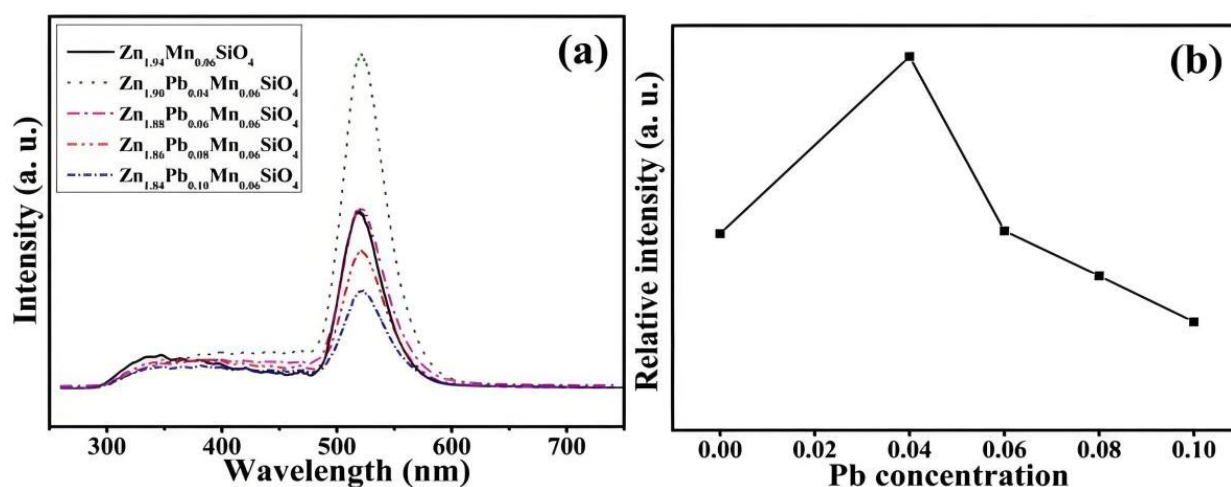
Fig. 4. (a) Emission spectra of $Zn_{1.94-x}Pb_xMn_{0.06}SiO_4$ with various Pb^{2+} ion concentrations (b) dependence of the emission intensity on the Pb^{2+} doping concentration (colour online)

The higher the Pb^{2+} ion concentration, the more significant the fluorescence intensity is exhibited. When the Pb^{2+} ion concentration is 0.4 corresponding to the highest luminescence intensity. This suggests that there is a non-radiative Pb^{2+}-Mn^{2+} energy transfer [21]. The luminescence intensity of the Mn^{2+} ion is increased at the expense of the luminescence quenching of the Pb^{2+} ion. After that, the higher the Pb^{2+} concentration, the emission intensity of peaks has greatly decreased due to energy migration to the neighboring Pb^{2+} ion in the system (Pb-Pb), which is attributed to the concentration quenching of the pb^{2+}.

3.4. Luminescence mechanism analysis

The luminescent mechanism of Pb^{2+}, Mn^{2+} co-doped Zn_2SiO_4 can be described as follows: the Zn_2SiO_4 matrix absorbs photons, leading to the excitation of electrons from the valence band to the conduction band, where they become trapped by defects. The recombination process involves both defect states and excited states of the Mn^{2+} and Pb^{2+} ions, resulting in observable visible emissions. During this luminescent process, the Pb^{2+} ion is initially excited; subsequently, energy transfer occurs from Pb^{2+} to Mn^{2+}. Following this transfer, various excited states of the Mn^{2+} ion decay radiatively back to its ground state ($6S^6$). Consequently, the emission spectrum depicted in Fig. 4a can be attributed to the *d-d* transition of the Mn^{2+} ion.

4. Conclusion

In summary, Mn^{2+} and Pb^{2+} co-doped Zn_2SiO_4 have been successfully prepared using mesoporous silica SBA-15 as an active template and silicon source. The effect of different Pb^{2+} percentage doping on physical, structural, optical and luminescent performance have been studied in detail. The structural characterization verifies the crystalline phases of $Zn_{1.94-x}Pb_xMn_{0.06}SiO_4$ ($0.04 \leq x \leq 0.10$) can be attributed to the diffractions of the pure willemite Zn_2SiO_4. The emission peak originates from the *d-d* jump of the Mn^{2+} ion and the luminescent properties show a dependence on the concentration of the Pb^{2+} ion. In all of the co-doped samples, the Pb^{2+} ion concentration of 0.4 corresponds to the highest luminescent intensity. The higher the Pb^{2+} concentration, the greater the fluorescence quenching. It is expected that this strategy can be applied to fabricate other luminescence materials.

References

[1] J. Shi, X. Sun, L. Song, M. Hong, Q. Yuan, Y. Zhang, Prog. Mater. Sci. **142**, 101246 (2024).

[2] P. Diana, S. Sebastian, D. Sivaganesh, C. S. A. Raj, S. Santhosh Kumar Jacob, T. H. AlAbdulaal, M. Shkir, Radiat. Phys. Chem. **212**, 111156 (2023).

[3] T. I. Krasnenko, A. N. Enyashin, N. A. Zaitseva, R. F. Samigullina, A. P. Tyutyunnik, I. V. Baklanova, M. V. Rotermel, T. A. Onufrieva, J. Alloy. Compd, **820**, 153129 (2020).

[4] T. I. Krasnenko, R. F. Samigullin, N. A. Zaitseva, I. I. Ivanova, S. V. Pryanichnikov, M. V. Rotermel, T. A. Onufrieva, J. Alloy. Compd, **907**, 164433 (2022).

[5] S. A. A. Wahab, K. A. Matori, S. H. A. Aziz, M. H. M. Zaid, M. M. A. Kechik, I. R. Ibrahim, M. Z. A. Khiri, N. Effendy, M. N. Abu Bakar, J. Alloy. Compd, **926**, 166726 (2022).

[6] B. C. Babu, B. V. Rao, M. Ravi, S. Babu, J. Mol. Struct. **1127**, 6 (2017).

[7] H. Liu, D. Moronta, L. Li, S. Yue, S. S. Wong, Phys. Chem. Chem. Phys. **20**, 10086 (2018).

[8] M. H. M. Zaid, K. A. Matori, S. H. A. Aziz, H. M. Kamari, I. Ismail, N. F. Samsudin, S. S. A. Rashid, J. Mater. Sci.: Mater. Electron. **28**,12282 (2017).

[9] P. Diana, S. Sebastian, S. Saravanakumar, M. C. Robert, M. Shkir, Ceram. Int. **49**, 26469 (2023).

[10] C. Yoon, S. Kang, J. Mater. Res. **16**, 1210 (2001).

[11] L. Dang, C. Tian, S. Zhao, Q. Lu, J. Cryst. Growth **491**, 126 (2018).

[12] L. Wang, J. Xiang, C. Li, C. Leung, J. Xiang, Front. Chem. **9**, 636431 (2021).

[13] J. Pejchal, E. Mihokova, M. Nikl, A. Novoselov, A. Yoshikawa, Opt. Mater. **31**, 1673 (2009).

[14] M. Yılmaz, E. Erdogmus, J. Lumin. **218**, 116868 (2020).

[15] O. Nazarenko, M. R. Kotyrba, S. Yakunin, M. Aebli, G. Rainò, B. M. Benin, M. Wörle, M. V. Kovalenko, J. Am. Chem. Soc. **140**, 3850 (2018).

[16] C. Peng, Z. Zhuang, H. Yang, G. Zhang, H. Fei, Chem. Sci. **9**, 1627 (2018).

[17] J. Wang, L. Gao, J. Zhang, L. Zhao, X. Wang, X. Niu, L. Fan, T. Hu, Cryst. Growth Des. **19**, 630 (2019).

[18] Q. Lu, P. Wang, J. Li, Mater. Res. Bull. **46**, 791 (2011).

[19] H. Wang, Y. Ma, G. Yi, D. Chen, Mater. Chem. Phys. **82**, 414 (2003).

[20] T. Baskaran, J. Christopher, T. G. Ajithkumar, A. Sakthivel, Appl. Catal. A-Gen. **488**, 119 (2014).

[21] S. Wang, M. Lü, F. Gu, Y. Qi, D. Xu, D. Yuan, D. Cao, Appl. Phys. A. **80**, 871 (2005).

[22] T. I. Krasnenko, N. A. Zaitseva, I. V. Ivanova, I. V. Baklanova, R. F. Samigullina, M. V. Rotermel, J. Alloy. Compd. **845**, 156296 (2020).

[23] T. S. Ahmadi, M. Haase, H. Weller, Mater. Res. Bull. **35**, 1869 (2000).

[24] P. Dai, Z. Xu, X. Yu, Y. Wang, L. Zhang, G. Li, Z. Sun, X. Liu, M. Wu, Mater. Res. Bull. **61**, 76 (2015).

_____
*Corresponding author: danglyhebeinu@163.com; yangzhenxing2017@163.com